16th World Conference on Earthquake Engineering, 16WCEE 2017

Santiago Chile, January 9th to 13th 2017

Paper N° 3908

Registration Code: S-S1464746185

STUDY ON SEISMIC BEHAVIOR OF CABLE RACK SYSTEM FOR ELECTRIC WIRING HAVING PASSIVE CONTROL SCHEME

K. Matsuda[(1)], K. Kasai[(2)]

[(1)] *Assistant Professor, Tokyo Institute of Technology, matsuda.k.aa@m.titech.ac.jp*
[(2)] *Professor, Tokyo Institute of Technology, kasai.k.ac@m.titech.ac.jp*
…

Abstract

Hanging type cable rack system partially had serious damage during the Tohoku-oki Earthquake, March 11, 2011. The objective of this paper is to understand the seismic performance of the cable lack system and to propose passive control scheme for the system. Monotonic loading tests of the cable rack and shake table tests of hanged cable rack are conducted. Performance of the specimens is discussed by referring to maximum deformations, displacements, absolute accelerations, relationships of damper force and damper deformation

Keywords: Shake Table Test; Member-by-Member Analytical Model; Visco-elastic Damper

1. Introduction

Many kinds of nonstructural components had serious damage during the Tohoku-oki Earthquake, March 11, 2011 and 68% of the damage report of electrical wiring was occupied by the hanging type cable rack system. The cable rack system is used to distribute the electric wiring in various buildings in Japan. In the case of large-scale facilities, the mass of the cable becomes 100 kg/m at most, the collapse of the cable rack system has a possibility of loss of human life. Moreover it is important to mitigate the damage of the cable rack system in order to recover from seismic damage early. However there are few past research[1)], the dynamic behavior of the cable rack system is not made known. The objective of this paper is to understand the seismic performance of the cable lack system and to propose passive control scheme for the system.

2. Cable Rack System

The cable rack system is member for wiring electric cable and transmission cable, is suitable for wiring a large amount of cable. Fig. 1 indicates the outline of the cable rack system. The horizontal plane is composed of main-beam and sub-beam in a reticular pattern, the beams are partially welded each other. The hanging bolt is connected to inserted nut on slab or metallic member on steel frame, and supports the weight of the cable rack.

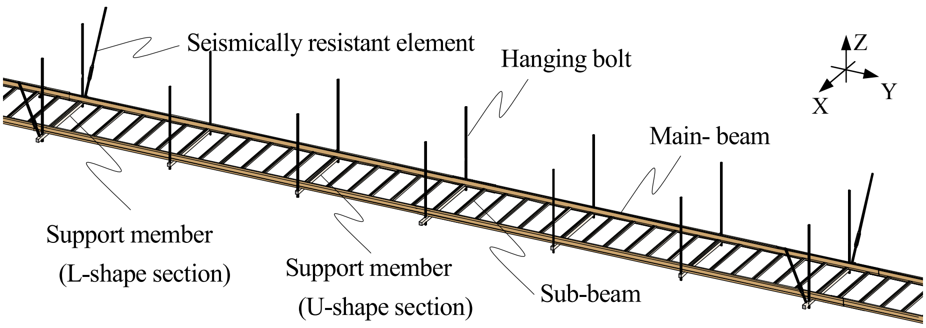

Fig. 1 – Outline of cable rack system

Seismically resistant element should be configured at 12-meter intervals at least. In this paper, the distance between two main beams is 1,000mm as large scale type, the length of hanging bolt is also 1,000mm, the responses for x direction (Fig. 1) will be discussed.

3. Horizontal Plane Test

3.1 Test schemes

In order to understand the mechanical behavior of the horizontal plane, a static test of the horizontal plane was carried out. Fig. 2 indicate setup image and overview of the static test. Total length of the specimen is 6,000mm, the lying specimen is vertically sandwiched by eight steel members with teflon (low friction) sheet to restrain out-of-plane deformation. Reaction force are supported by two roller bearings which have 4,500mm distance each other, there are two loading point at a distance of 900mm. Basically the specimen are subjected to monotonic loading, but the load is reduced to 0kN at 15, 30, 60 and 90mm deformation to understand unloading stiffness.

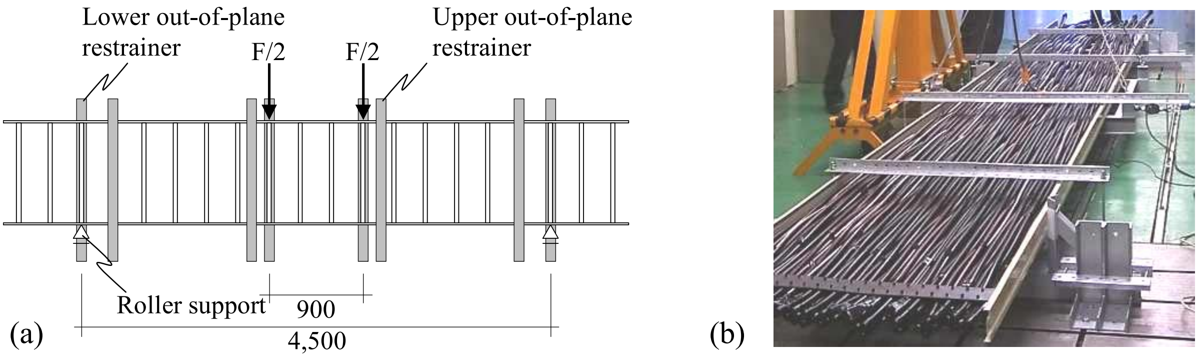

Fig. 2 – Static test of cable rack, (a) Outline, (b) Outview

Total number of the specimen is three (indicated in Table 1), the parameter is the presence or absence of cable, in the case of presence of cable, there are two types of nylon band distance 1,500mm and 2,700mm to fasten the cable and sub beam. At the both edge of the specimen, all cables are fixed by steel plates in order to restrain the cable slide of axial direction assuming sufficiently long cable rack.

Fig. 3 illustrates measurement scheme. 4,500mm area is split to five areas, absolute displacement of loading direction and relative displacement of diagonal position are measured in each area. Total deformation angle θ_j and shear deformation angle γ_j at area j are obtained from equation (1) and (2) respectively.

$$\theta_j = \left|\delta_{j+1} - \delta_j\right| / 900 \tag{1}$$

$$\gamma_j = \frac{\left({}_j\delta_1 - {}_j\delta_2\right)\sin\alpha}{1800 + \left({}_j\delta_1 + {}_j\delta_2\right)\cos\alpha} + \frac{\left({}_j\delta_1 - {}_j\delta_2\right)\cos\alpha}{2000 + \left({}_j\delta_1 + {}_j\delta_2\right)\sin\alpha} \tag{2}$$

Table 1 – Parameter of cable rack

Name	2700	1500	No
Cable	○	○	×
Nylon band distance	2700	1500	×

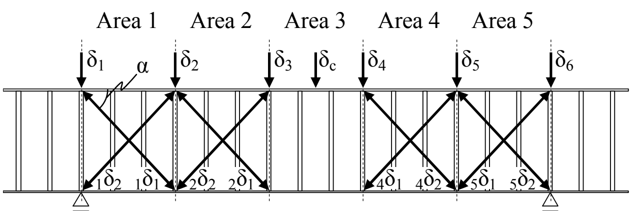

Fig. 3 – Measurement scheme of horizontal plane test

3.2 Test results

During loading test, the welded connections between main- and sub-beam were mainly broken as the deformation progressed. The relationship between load F and center displacement u_c is shown in Fig. 4. The envelop curves don't have clear yield point, the stiffness is gradually decreasing as the deformation progressed. Although specimen "1500" and "2700" with cable have almost 10% higher stiffness than specimen "No" without cable, the two specimen "1500" and "2700" were not different clearly each other. It is assumed that the effective of the nylon band is not significant for mechanical behavior of the cable rack.

Taking specimen "2700" for example, the relationships between total deformation angle θ_j and shear deformation angle γ_j are shown in Fig. 5. In all areas, the shear deformation angle γ_j was almost same as the total deformation angle θ_j and the other specimens also have same tendency. Therefore, the shear deformation would be dominant for the cable rack of this research subject.

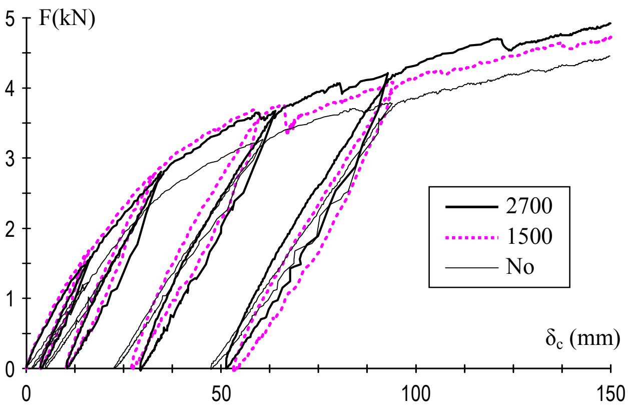

Fig. 4 – F - δ_c relationships

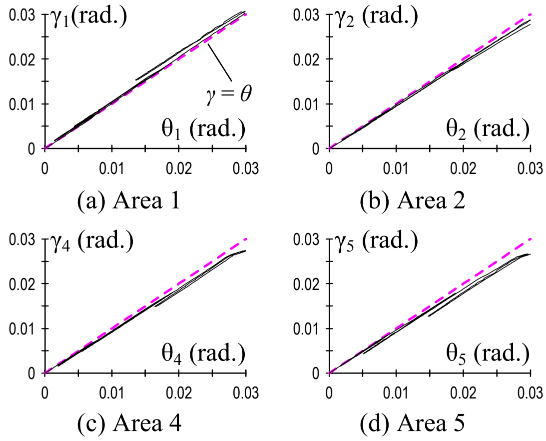

Fig. 5 – γ_n - θ_n relationships (specimen 2700)

4. Shake Table Test Schemes

4.1 Outline and specimen parameter

Assuming sufficiently long cable rack system which has seismically resistant element at intervals of 10.8m, as shown in Fig. 6. The specimen is 5.4m area which is picked out from long cable rack system in consideration of symmetric property. The cable rack is supported by hanging bolts and support members at intervals of 1.8m. All cables are fastened by nylon band at intervals of 2,7m. All cables are fixed by steel plates in order to restrain the cable slide of axial direction same as chapter 3. The weight per meter of the cable and cable rack are 97.2kg/m and 8.9kg/m respectively, and total weight is 637kg. Parameter of the specimen is

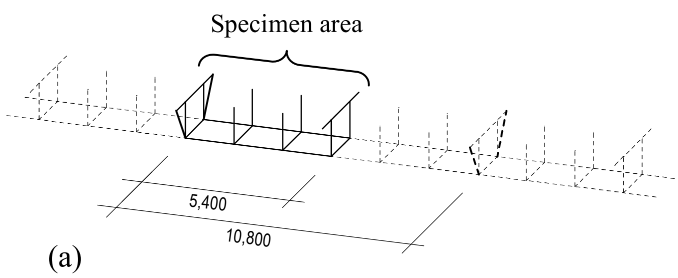

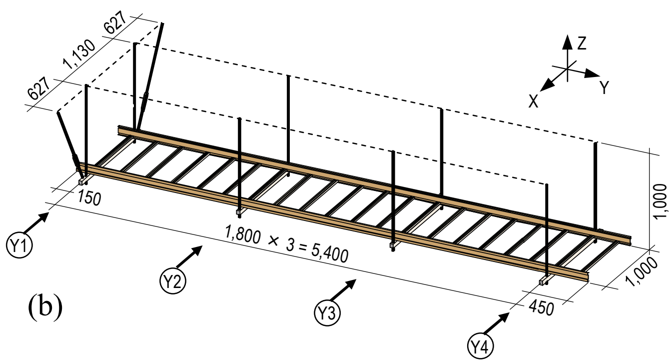

Fig. 6 – Specimen for shake table test, (a) Picking up test area, (b) Detail size of specimen

seismic resistant element type of Y1- and Y4-plane.

In this study, there are three types of the seismic resistant element as shown in Fig. 7, specimen having standard seismic braces which are composed of turn buckle (Fig. 7(a)), specimen having viscoelastic dampers instead of braces (Fig. 7(b)) and specimen having a viscoelastic damper between two hanging bolts for seismic retrofitting (Fig. 7(c)). In the case of having viscoelastic damper, the hanging bolts are covered to prevent the bolt from buckling, and there are resinous type spacers between the cover and the bolt. The damper is composed of 5mm thickness viscoelastic material between outer- and inner-cylinder, and the damper is connected in series by M6 screws in order to make actual thickness 10mm. The letters of Br mean Brace, VE means Visco-Elastic, R means Retrofit and Co means Cover.

Specimen parameter of the shake table test is listed in Table 2. Specimen "Br-No" has seismic brace at Y1-plane, it meets the required criteria of the seismic element at least. Specimen "Br-Br" has seismic brace also at Y4-plane, specimen "Br-VE" and "Br-VE(R)" have visco-elastic damper at Y4-plane in addition of "Br-No". The cable rack of specimen "Br(R)-VE(R)+Co" is retrofitted by 1.6mm thickness cover. But in the case of specimen "Br(R)-VE(R)+Co", the hanging bolt at Y1-plane is retrofitted to prevent the hanging bolt from buckling.

As input table motion, BCJ-L2 is used. BCJ-L2 is artificial motion producing constant pseudo-velocity of 148 cm/s at 2% damping ratio, and the motion will be scaled 0.1, 0.3, 0.5, 0.7, 1.0, and 1.7 times, in order to compare the performance at various seismic levels.

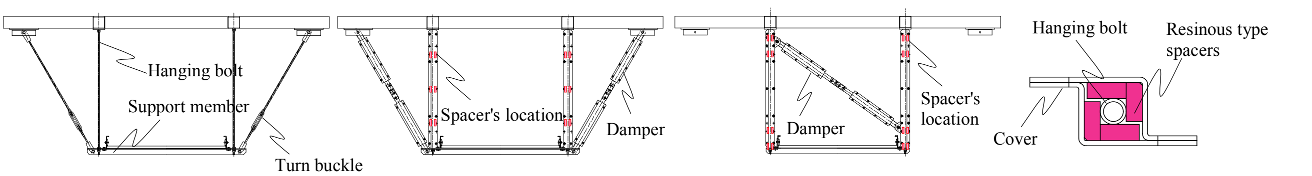

(a) Br plane (b) VE plane (c) VE(R) plane (d) Cross section of reinforced bolt

Fig. 7 – Seismic resistant element

Table 2 – Parameter of shake table test

Name	Br-No	Br-Br	Br-VE	Br-VE(R)	Br(R)-VE(R)+Co
Vib. Period	0.706 sec	0.319 sec	0.322 sec	0.324 sec	0.234 sec
Damping Ratio	2.5%	2.9%	4.1%	4.2%	5.1%
VE shear area	—	—	$100cm^2 \times 2$	$150cm^2$	$150cm^2$
Cover	—	—	—	—	○
Configuration	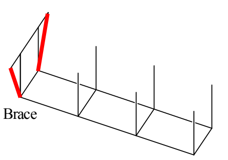	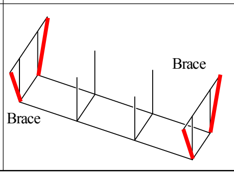	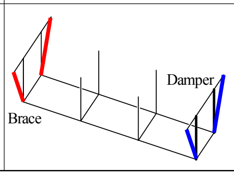	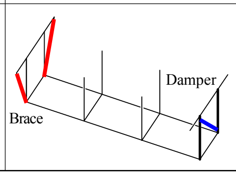	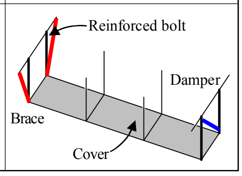

Note: Vibration period & damping ratio are calculated from curve fitting method of transfer function under first BCJ-L2 10% [2)]

4.2 Setup

Setup of the shake table test is shown in Fig. 8. A hanging frame which has 50 Hz natural frequency is fixed to a shake table, the cable rack is hanged from the hanging frame. In order to replicate realistic condition, a jig to fix rotation behavior about the Z axis is installed around Y1 plane (Fig 9). Two ball casters sandwich the main beam with fixed member on both side. Clearance between the two ball caster is able to be adjust by thin steel plate, and is thinner than 0.7mm. The turn buckle is fasten in 1 kN before first shaking.

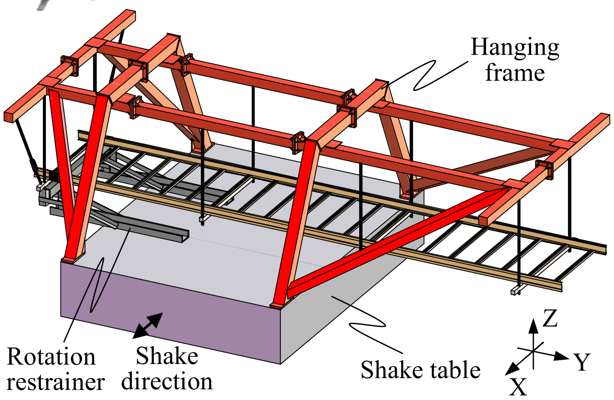

Fig. 8 – Setup for shake table test

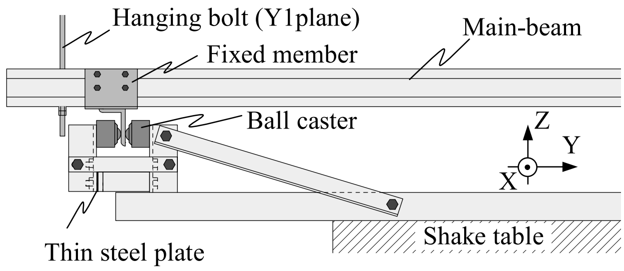

Fig. 9 – Detail of rotation restrainer

4.3 Measurement scheme

Measurement scheme of the shake table test is shown in Fig. 10. Two acceleration sensors are installed at both ends of the shake table ($\ddot{u}_{g1}, \ddot{u}_{g2}$). As a global behavior of the specimen, relative displacement (u_1 ~u_4) and absolute acceleration ($\ddot{u}_{tot1}$ ~ $\ddot{u}_{tot4}$) of from Y1 plane to Y4 plane are measured in X axis direction. To understand the rotation angle about the Z axis of the specimen, two displacements of Y axis direction at Y1 plane are measured (δ_{y1}, δ_{y2})。

Damper force (F_d) is obtained from average of the two strain gages which are pasted in inner-cylinder. Damper deformation (u_d) is measured at four points and added component deformation (u_a) which includes not only damper deformation bat also cylinder and connection are measured at two points. Temperature of the visco-elastic material is measured by thermocouple, the temperature is adjusted at 20 ± 0.2 degrees C before each shaking. Bending moment and axial force of the hanging bolt are measured by strain gages which are pasted at two points 400mm away.

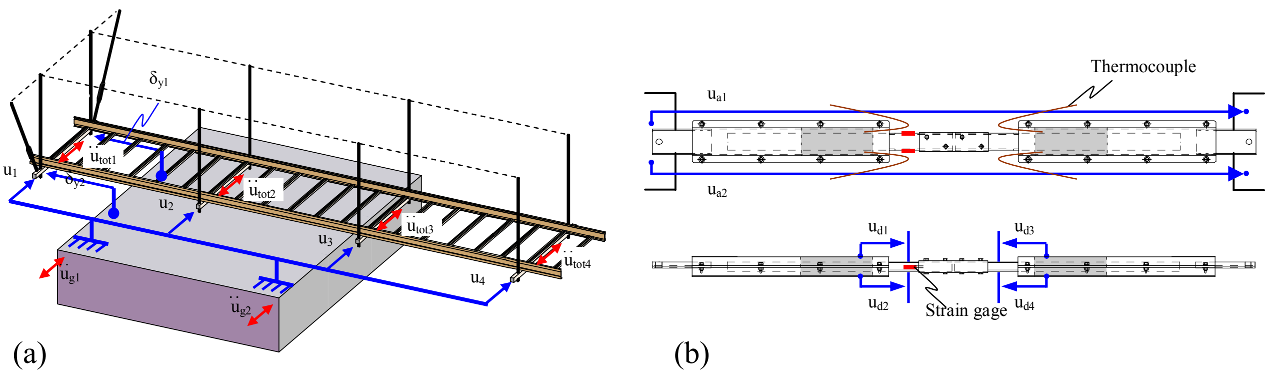

Fig. 10 – Measurement scheme, (a) Glorbal measurement, (b) Local measurement

5. Shake Table Test Results

5.1 Force equilibrium

Fig. 11 illustrates dynamic model of the shake table test. The masses (m_i) are concentrated four points and inertia force ($F_{inertia}$) is obtained from equation (3a). Spring force (F_{spring}) is obtained from equation (3b) as summation of each plane spring force for X axis direction. F_{hi} is summation of shear force of the hanging bolt (Q_{bi}) and pendulum force (F_{pi}) as shown in equation (3c), F_{bi} is horizontal component of brace or damper force. Q_{bi} is obtained from strain gages and F_{pi} is calculate from equation (3d)。 Figure 10 shows comparison between

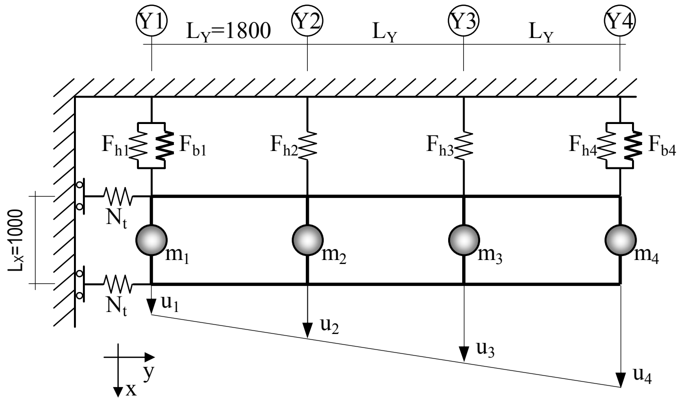

Fig. 11 – Dynamic model of shake table test

$F_{inertia}$ and F_{spring} for the specimen Br-VE(R) under the 100% BCJ-L2 motion. It is confirmed that all measurement has high accuracy because the two forces match well as shown Fig. 12.

$$F_{inetia} = \sum_{i=1}^{4} m_i \ddot{u}_{toti} \quad , \quad F_{spring} = \sum_{i=1}^{4} (F_{hi}) + F_{b1} + F_{b4} \quad , \quad F_{hi} = Q_{bi} + F_{pi} \quad , \quad F_{pi} = m_i g \cdot u_i / L_b \tag{3a-d}$$

Over turning axial force N_t is calculated from over turning moment M_t as shown in equation (4). The relationship between N_t and δ_y of specimen Br-No under 100% BCJ-L2 motion is shown in Fig. 13. The gap area was not so large and stiffness is almost 5kN/mm. N_t of specimen Br-No which has seismic resistant element in only Y1 plane is largest, and the rotation angle is up to just 3.6×10^{-3} under 170% BCJ-L2 motion.

$$M_t = \sum_{i=1}^{4} \left[(m_i \ddot{u}_{toti} - F_{hi} - F_{bi})(i-1) L_y \right] \quad , \quad N_t = M_t / L_x \tag{4a, b}$$

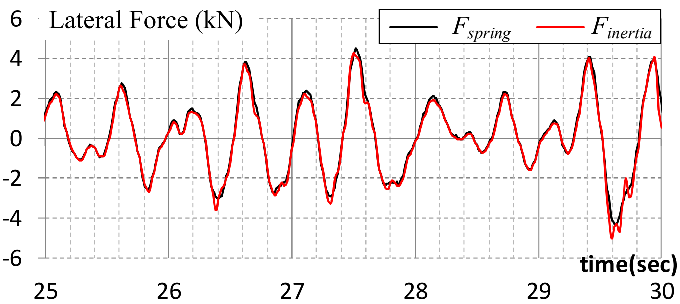

Fig. 12 – Comparison between F_{spring} and $F_{inertia}$

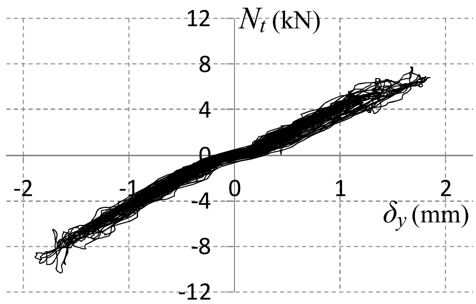

Fig. 13 – Relationship of N_t and δ_y

5.2 Peak responses

Fig. 14 indicates peak responses of displacement, acceleration and deformation of each plane and area. Specimen Br-No which has seismic braces at only Y1 plane had the largest displacement and deformation, when specimen Br-No was subjected to BCJ-L2 170%, the displacement of Y4 plane is 232mm. In the case of specimen Br-Br which has seismic brace at also Y4 plane, both displacement and deformation were much smaller than specimen Br-No, however its acceleration was the largest of all specimens. Although specimens Br-VE and Br-VE(R) which have visco-elastic damper at Y4 plane instead of seismic brace had smaller acceleration than specimen Br-Br, deformation of area Y1-Y2 was larger than Br-Br a little. Therefore if

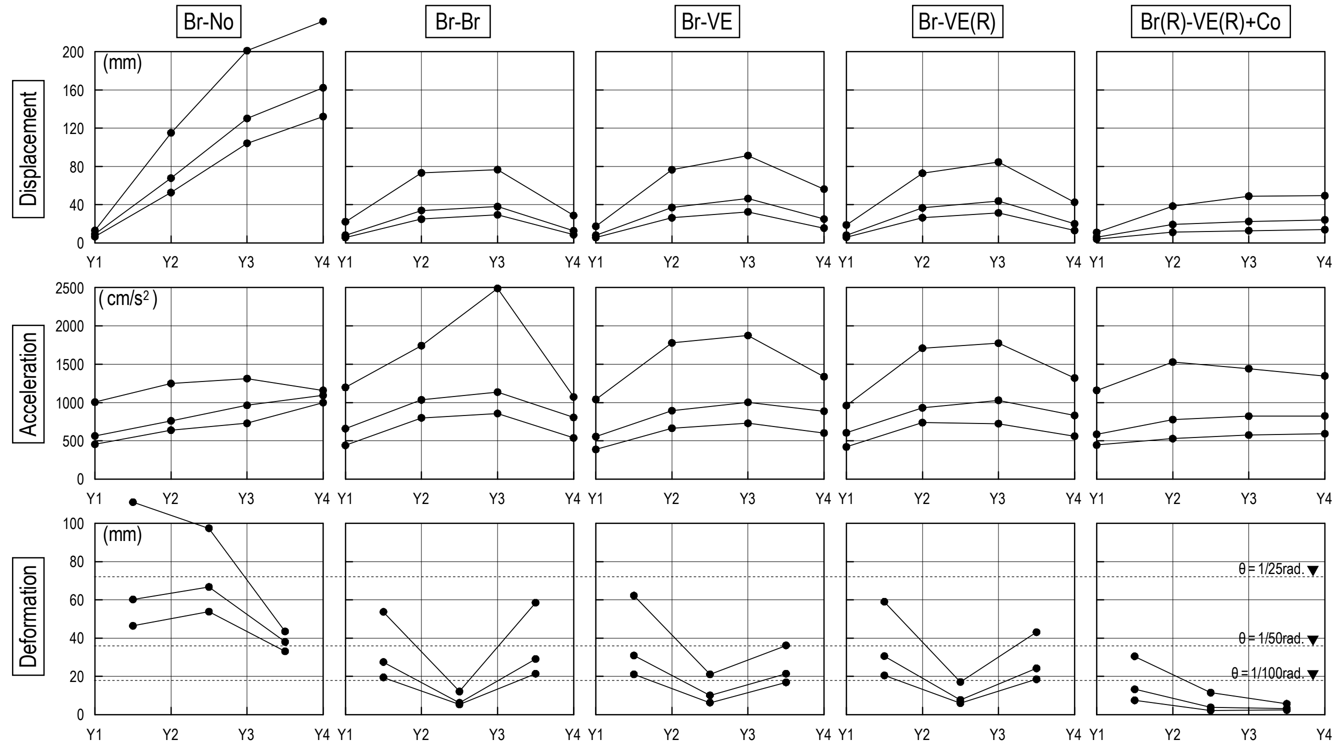

Fig. 14 – Peak responses of all specimens (From lower side BCJ-L2 70%, 100%, 170%)

seismic braces of dampers are installed at Y4 plane, the displacement of Y4 plane becomes small, but it is difficult to control displacement of Y2 and Y3 plane and deformation. The hanging bolt and seismic brace of Y1 plane buckle and have damage after BCJ-L2 170% especially. In order to control the deformation and damage, the cable rack of specimen Br(R)-VE(R)+Co were covered and hanging bolts were restrained for buckling, same as hanging bolts of damper plane. The displacement and deformation of specimen Br(R)-VE(R)+Co were controlled obviously.

5.3 Hysteresis of brace and damper

Fig. 15 shows the relationships between damper force F_d and damper deformation u_d under BCJ-L2 170%. Each graphs also show theoretical curve [3)] of damper material which is calculated by damper temperature, maximum shear strain and vibration period. The properties of the ellipsoid are obtained from next equations.

$$G_{eq} = aT\left(A1\,\omega^{A2}\gamma^{A3}\right) \;,\; C_{eq} = bT\left(B1\,\omega^{B2}\gamma^{B3}\right) \tag{5a, b}$$

$$aT = \exp\left(A4\left(Temp-20\right)/\left(Temp+273\right)\right) \;,\; bT = \exp\left(B4\left(Temp-20\right)/\left(Temp+273\right)\right) \tag{6a, b}$$

Where, Geq, Ceq are shear elastic modulus and equivalent damping coefficient per unit area respectively, ω is circular frequency, γ is shear strain, Temp is temperature and A1～A4, B1～B4 are constant number[3)].

As shown in Fig. 15, when the specimens are subjected to BCJ-L2 170%, the shear strain γ was up to 250%, then the temperature rise was within 10 degree. All hystereses were stably ellipsoid shape, and it is clear that the dampers absorbed the seismic energy effectively. The dampers behaved as expected because the theoretical ellipsoids contain the hystereses of test result.

Fig. 16 shows the relationships between axial force and axial deformation of seismic brace under BCJ-L2 170%. The seismic brace buckled obviously because the tensile side stiffness is higher than the compression

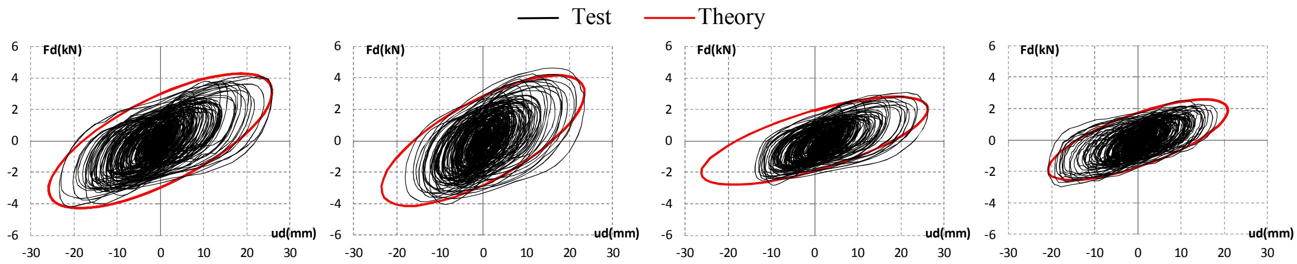

(a) Br(R)-VE(R)+Co (b) Br-VE(R) (c) Br-VE (F_{d1}-u_{d1}) (d) Br-VE (F_{d2}-u_{d2})

Fig. 15 – Relationships between axial damper force and deformation

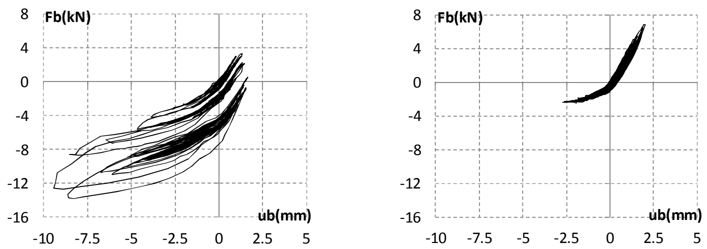

(a) Br-Br (b) Br(R)-VE(R)+Co)

Fig. 16 – Relationships between axial brace force and deformation

side stiffness in both graphs. In the case of specimen Br-Br, axial force shift to negative side, it means the brace was plasticized at strain gage point. On the other side, brace of specimen Br(R)-VE(R)+Co keeps elastic situation even if after BCJ-L2 170%.

6. Conclusions

1) Monotonic loading tests of the cable rack are conducted using full-size specimen with/without cable and their deformation mode and non-linearity are figured out. It is clear that the deformation is almost occupied by shear deformation.

2) Shake table tests of hanged cable rack are conducted. It is difficult to reduce displacement and deformation of the cable rack by using only seismic brace under BCJ-L2 170%. Cable rack cover is effective to reduce the deformation of the cable rack.

3) The visco-elastic damper stably had ellipsoid shape hysteresis, and it is clear that the dampers absorbed the seismic energy effectively. The dampers behaved as expected because the theoretical ellipsoids contain the hystereses of test result.

7. References

[1] Sumi, A., Teramoto, T., Ohmiya, M. and Shinozaki, M: Research on the Seismic Resistance of Electric Cable Racks, The Journal of the Institute of Electrical Installation Engineers of Japan, Vol. 24, No. 10, pp.804-810, 2004.10 (In Japanses)

[2] Kasai, K., Mita, A., Kitamura, H., Matsuda, K., Morgan, T. and Taylor, A.: Performance of Seismic Protection Technologies During the 2011 Tohoku-Oki Earthquake, Earthquake Spectra, Special Issue on the 2011 Tohoku-Oki Earthquake and Tsunami, pp.265-294, 2013.3

[3] Nomura, T., Kohara, K. and Senda, S.: Development of Visco-Elastic Structural Control Dampers for Timber Houses - Part 1. Dynamic Properties of Brace Type, Proc. Annual Meeting of Architectural Institute of Japan, C-1, pp. 469-470, 2009.7 (In Japanses)